

## Supporting Information

### ***In Situ* Coupling of Co<sub>0.85</sub>Se and N–Doped Carbon via One–Step Selenizing of Metal–Organic Frameworks as Trifunctional Catalysts for Overall Water Splitting and Zn–air Batteries**

*Tao Meng, Jinwen Qin, Shuguang Wang, Di Zhao, Baoguang Mao, Minhua Cao\**

Key Laboratory of Cluster Science, Ministry of Education of China, Beijing Key Laboratory of Photoelectronic/Electrophotonic Conversion Materials, School of Chemistry and Chemical Engineering, Beijing Institute of Technology, Beijing 100081, P. R. China.

\*E-mail: caomh@bit.edu.cn

## 1. Supplementary figures

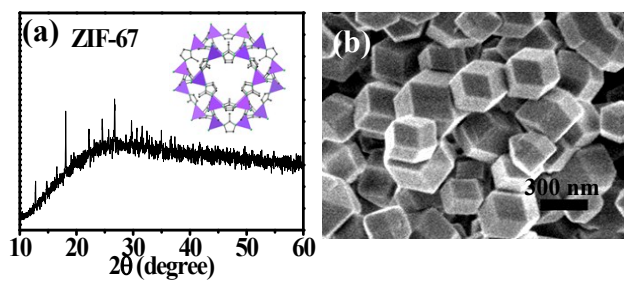


**Fig. S1** (a) XRD pattern and (b) FE-SEM image of ZIF-67.

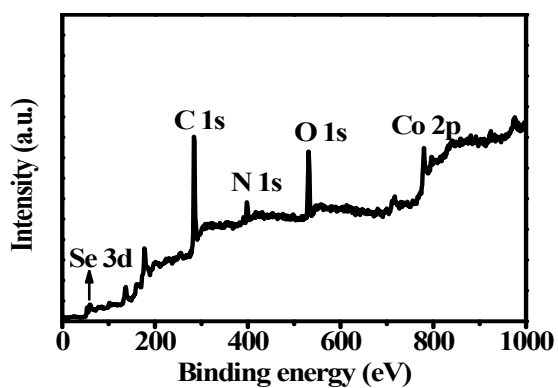


**Fig. S2** The survey XPS spectrum of  $\text{Co}_{0.85}\text{Se}@\text{NC}$ .

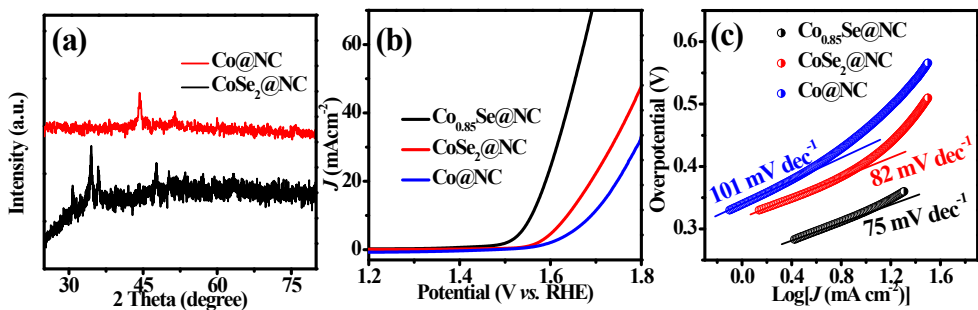


**Fig. S3** (a) XRD patterns for CoSe<sub>2</sub>@NC and Co@NC; (b) Polarization curves and (c) Tafel plots of Co<sub>0.85</sub>Se@NC, CoSe<sub>2</sub>@NC and Co@NC.

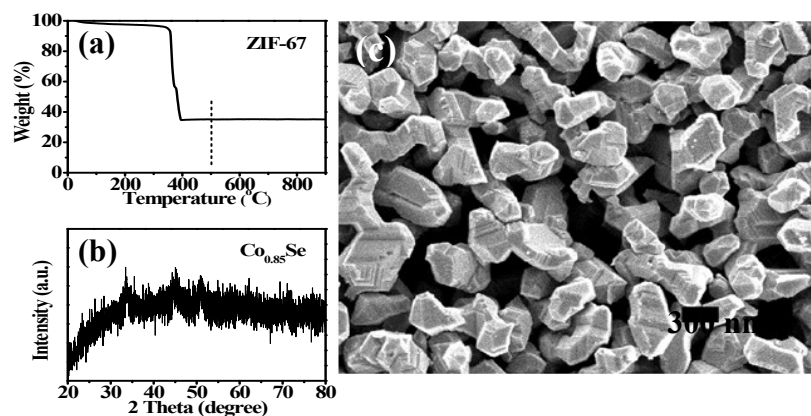


**Fig. S4** (a) The TGA curve of ZIF-67. (b) The XRD pattern and (c) FE-SEM image of Co<sub>0.85</sub>Se.

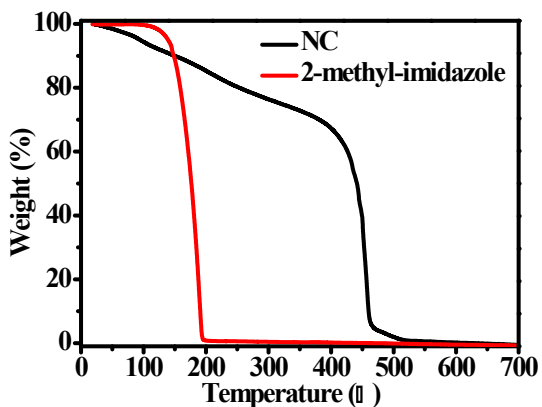


**Fig. S5** The TGA curves of NC and 2-methyl-imidazole.

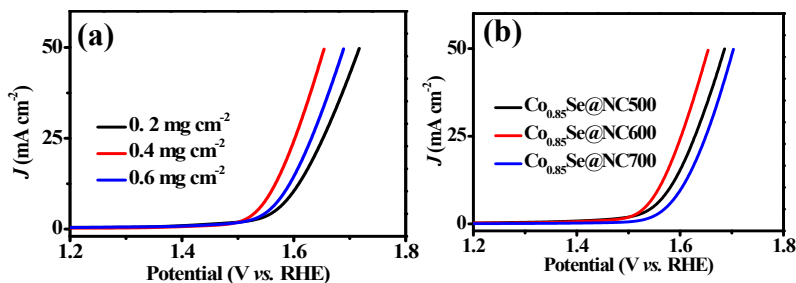


**Fig. S6** (a) Polarization curves of  $\text{Co}_{0.85}\text{Se}@NC$  coated on glass carbon (GC) electrode with different mass rates at  $2 \text{ mV s}^{-1}$ . (b) Polarization curves of  $\text{Co}_{0.85}\text{Se}@NC$  prepared with different temperatures.

**Fig. S6 (b):** The  $\text{Co}_{0.85}\text{Se}@NC500$  and  $\text{Co}_{0.85}\text{Se}@NC700$  both exhibit slightly inferior oxygen evolution activity, which is probably due to either the poor crystallinity at the low temperature or the aggregation of  $\text{Co}_{0.85}\text{Se}@NC$  nanocrystallites at the high temperature.

**Table S1** Comparison of the OER activity for several recently reported highly active transition-/noble-metal and non-metal catalysts supported on different substrates.

Catalyst	Mass loading (mg cm <sup>-2</sup> )	Potential @ 10.0 mA cm <sup>-2</sup> (V vs. RHE)	Tafel slope (mV dec <sup>-1</sup> )	Electrolyte	Substrate	Ref.
<b>Co<sub>0.85</sub>Se@NC</b>	<b>0.4</b>	<b>1.55</b>	<b>75</b>	<b>1 M KOH</b>	<b>Glassy carbon</b>	<b>This work</b>
IrO <sub>2</sub> /C	0.2	1.60	N.A.	0.1 M KOH	Glassy carbon	1
Pt/C	~0.25	1.83	169	0.1 M KOH	Glassy carbon	2
CoSe <sub>2</sub> ultrathin nanosheets	0.142	1.55	44	0.1 M KOH	Glassy carbon	3
CoSe <sub>2</sub> /N-graphene	~0.2	1.596	~40	0.1 M KOH	Glassy carbon	4
Mn <sub>3</sub> O <sub>4</sub> /CoSe <sub>2</sub> hybrids	~0.2	1.68	49	0.1 M KOH	Glassy carbon	5
CoS <sub>2</sub> /N,S-GO	0.25	1.61	75	0.1 M KOH	Glassy carbon	6
Co <sub>3</sub> O <sub>4</sub> /N-graphene	1	1.54	67	1 M KOH	Ni foam	7
Co <sub>3</sub> O <sub>4</sub> C-NA	~0.2	1.52	70	0.1 M KOH	Cu foil	8
TCCN	~1.4	1.65	74.6	0.1 M KOH	self-supported membrane	9
CoP	6.2	1.52	65	1 M KOH	Ni foam	10
Zn <sub>x</sub> Co <sub>3-x</sub> O <sub>4</sub> nanoarrays	~1	1.55	51	1 M KOH	Ti foil	11
Ni <sub>x</sub> Co <sub>3-x</sub> O <sub>4</sub> nanoarrays	N.A.	~1.6	59-64	1 M NaOH	Ti foil	12

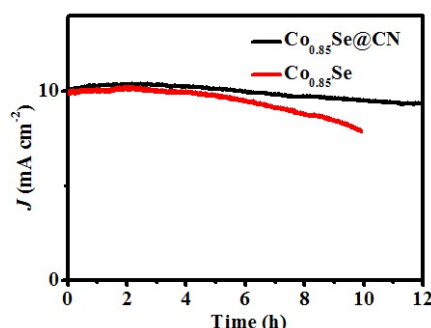


**Fig. S7** Chronoamperometric responses at a constant potential (the potential at 10 mA cm<sup>-2</sup>) of Co<sub>0.85</sub>Se@NC and Co<sub>0.85</sub>Se.

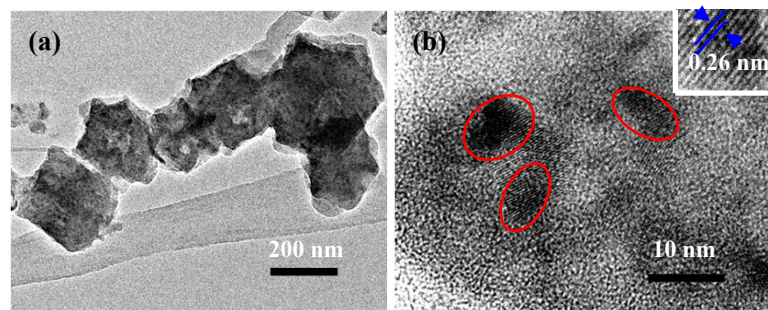


**Fig. S8** (a) TEM image and (b) HRTEM image of  $\text{Co}_{0.85}\text{Se}@\text{NC}$  after 12 h reaction.

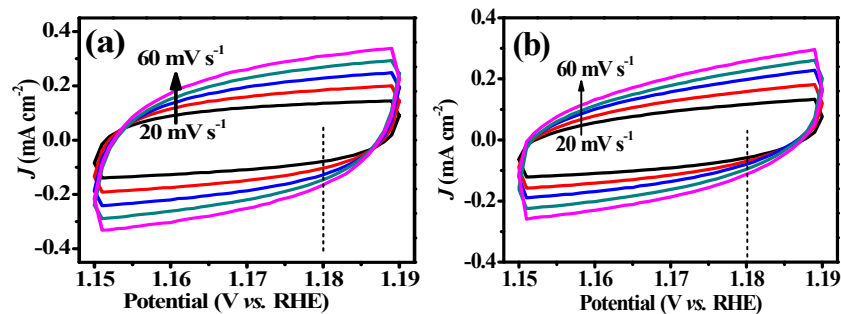


**Fig. S9** CVs tested at the potential range of 1.15–1.19 V vs. RHE with the scan rates increasing from 20 to 60  $\text{mV s}^{-1}$  for  $\text{Co}_{0.85}\text{Se}@\text{NC}$  (a) and  $\text{Co}_{0.85}\text{Se}$  (b).

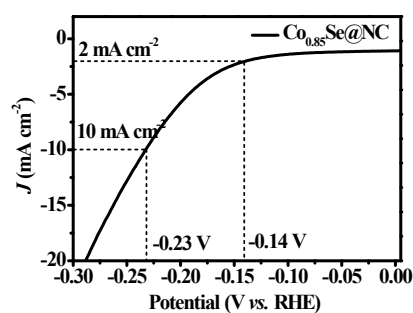


**Fig. S10** Polarization curve of  $\text{Co}_{0.85}\text{Se}@\text{NC}$  for HER ( $\text{N}_2$ -saturated 1.0 M KOH solution with a scan rate of 2  $\text{mV s}^{-1}$ ).

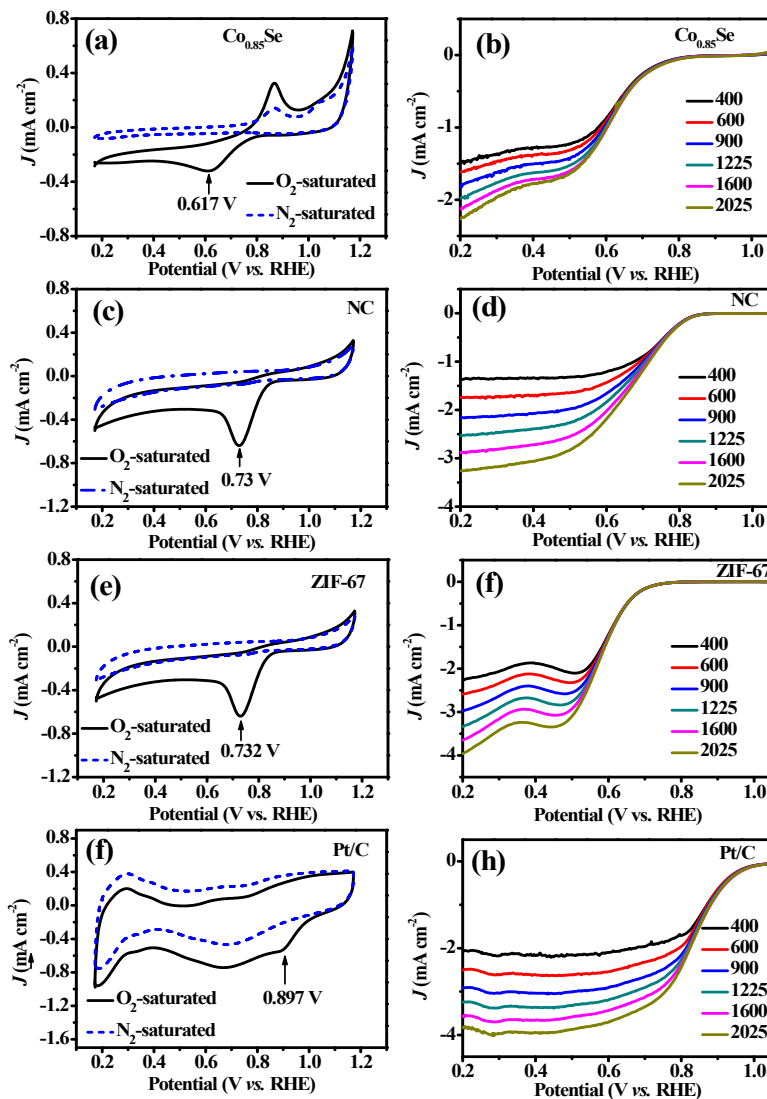


**Fig. S11** The CVs in  $0.1 \text{ M KOH}$  solution and polarization curves in  $\text{O}_2$ -saturated  $0.1 \text{ M KOH}$  solution with rotating speeds from 400 to 2025 rpm for  $\text{Co}_{0.85}\text{Se}$  (a,b), NC (c,d), ZIF-67(e,f) and Pt/C (g,h).

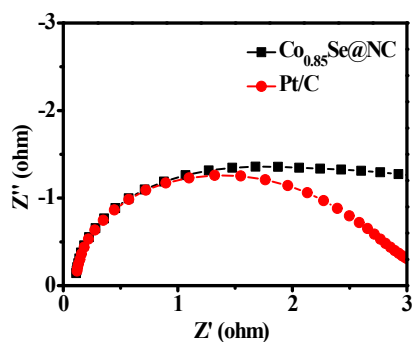


**Fig. S12** The EIS of  $\text{Co}_{0.85}\text{Se@NC}$  and commercial Pt/C at open-circuit voltage for Zn-air battery.

**Table S2** Comparison of the primary Zn–air batteries with several key parameters for several recently reported highly active transition–/noble–metal and non–metal catalysts.

ORR catalyst used	Zn electrode/electrolyte	Current density @ $V = 1.0$ V (mA cm $^{-2}$ )	Peak power density (mW cm $^{-2}$ )	Ref.
<b>Co<sub>0.85</sub>Se@NC</b>	<b>Zn foil/6M KOH</b>	<b>186</b>	<b>268</b>	<b>This work</b>
CoO/N–CNT	Zn foil/6 M KOH	197	265	13
Co@NG–acid	Zn foil/6 M KOH	255	350	14
Co <sub>3</sub> O <sub>4</sub> nanoparticles decorated carbon nanofiber	Zn plate/6 M KOH	81	125	15
Fe, Co and N precursors pyrolyzed with carbon	Zn plate/6 M KOH	150	232	16
Graphene supported Mn <sub>3</sub> O <sub>4</sub> nanoparticles	Zn power/(N.A.M) KOH	70	120	17
Ketjenblack carbon supported amorphous MnO <sub>x</sub>	Zn power/(6 M) KOH	120	190	18
Fe@N–C–700	Zn plate/6 M KOH	157	220	19
FeCu@GC	Zn plate/6 M KOH	100	212	20
Nanoporous carbon fiber films–1000	Zn plate/6 M KOH	~150	185	21
N–doped carbon nanotubes	Zn plate/6 M KOH	50	75	22
N,P–doped carbon foam	Zn plate/6 M KOH	<70	55	23

**Table S3** Comparison of the rechargeable Zn–air batteries with several key parameters for several recently reported highly active transition–/noble–metal and non–metal catalysts.

Air catalyst used	Cycling conditions and stability	Voltage polarization V (@ $j$ , mA cm $^{-2}$ )	Ref.
<b>Co<sub>0.85</sub>Se@NC</b>	<b>10 mA cm<math>^{-2}</math>, 600 s per cycle periods for 180 cycles: polarization increased ~0.16 V at the end</b>	<b>0.8 (10)</b>	<b>This work</b>
MnO <sub>2</sub> nanotube and carbon nanotube composite	~8 mA cm $^{-2}$ , 600 s per cycle periods for 50 cycles: polarization increased ~0.4 V at the end	1.5 (20)	24
Co <sub>3</sub> O <sub>4</sub> nanoparticles decorated carbon nanofibers	2 and 20 mA cm $^{-2}$ , 1 h per cycle periods for 160 and 55 cycles: polarization increased 0.09 V at the end for 20 mA cm $^{-2}$	0.7 (2) 0.85 (20)	15
Tri-electrode: CoO/N–CNT + NiFe LDH	20-50 mA cm $^{-2}$ , 4-20 h per cycle period for >200 h: negligible voltage change at the end	0.7 (20)	13
Co <sub>3</sub> O <sub>4</sub> NP modified MnO <sub>2</sub> nanotubes	15 mA cm $^{-2}$ ; 14 min per cycle period for 60 cycles; voltage gap increased ~0.3-0.4 V at the end	~0.85 (15)	25
ZnCo <sub>2</sub> O <sub>4</sub> /N–CNT	10-100 mA cm $^{-2}$ , 20 min per cycle for 17 cycles (340 min); negligible voltage change at the end	0.84(10-100)	26
TCCN	20 mA cm $^{-2}$ , 10 min per cycle for 15 cycles; negligible voltage change at the end	1.68 (20)	9

## 2. Supplementary video

**Video S.** Co<sub>0.85</sub>Se@NC coated on nikel foam was used as the working electrode for overall water splitting at the current density of 10 mA cm $^{-2}$ . This video instinctively reflects the generation rate of O<sub>2</sub> or H<sub>2</sub> gas with the Co<sub>0.85</sub>Se@NC catalyst during the overall water splitting, indicating its excellent overall water splitting performance.

### 3. References

- 1 Y. Zhao, R. Nakamura, K. Kamiya, S. Nakanishi and K. Hashimoto, *Nat. Commun.*, 2013, **4**, 2390—2396.
- 2 X. Lv, Y. Zhu, H. Jiang, X. Yang, Y. Liu, Y. Su, J. Huang, Y. Yao and C. Li, *Dalton Transactions*, 2015, **44**, 4148—4154.
- 3 Y. Liu, H. Cheng, M. Lyu, S. Fan, Q. Liu, W. Zhang, Y. Zhi, C. Wang, C. Xiao and S. Wei, *J. Am. Chem. Soc.*, 2014, **136**, 15670—15675.
- 4 M. R. Gao, X. Cao, Q. Gao, Y. F. Xu, Y. R. Zheng, J. Jiang and S. H. Yu, *ACS nano*, 2014, **8**, 3970—3978.
- 5 M. R. Gao, Y. F. Xu, J. Jiang, Y. R. Zheng and S. H. Yu, *J. Am. Chem. Soc.*, 2012, **134**, 2930—2933.
- 6 P. Ganesan, M. Prabu, J. Sanetuntikul and S. Shanmugam, *ACS Catalysis*, 2015, **5**, 3625—3637.
- 7 Y. Liang, Y. Li, H. Wang, J. Zhou, J. Wang, T. Regier, H. Dai, *Nat. Mater.*, 2011, **10**, 780—786.
- 8 T. Y. Ma, S. Dai, M. Jaroniec and S. Z. Qiao, *J. Am. Chem. Soc.*, 2014, **136**, 13925—13931.
- 9 T. Y. Ma, J. L. Cao, M. Jaroniec and S. Z. Qiao, *Angew. Chem. Int. Ed.*, 2016, **55**, 1138—1142.
- 10 Y. P. Zhu, Y. P. Liu, T. Z. Ren and Z. Y. Yuan, *Adv. Funct. Mater.*, 2015, **25**, 7337—7347.
- 11 X. Liu, Z. Chang, L. Luo, T. Xu, X. Lei, J. Liu, X. Sun, *Chem. Mater.*, 2014, **26**, 1889—1895.
- 12 Y. Li, P. Hasin, Y. Wu, *Adv. Mater.*, 2010, **22**, 1926—1929.
13. Y. G. Li, M. Gong, Y. Y. Liang, J. Feng, J. E. Kim, H. L. Wang, G. S. Hong, B. Zhang and H. J. Dai, *Nat. Commun.*, 2013, **4**, 1805—1811.
14. M. Zeng, Y. Liu, F. Zhao, K. Nie, N. Han, X. Wang, W. Huang, X. Song, J. Zhong and Y. Li, *Adv. Funct. Mater.*, 2016, **26**, 4397—4404.
15. B. Li, X. Ge, F. T. Goh, T. A. Hor, D. Geng, G. Du, Z. Liu, J. Zhang, X. Liu and Y. Zong, *Nanoscale*, 2015, **7**, 1830—1838.

16. Z. Chen, J. Y. Choi, H. Wang, H. Li and Z. Chen, *J. Power Sources*, 2011, **196**, 3673—3677.
17. J. S. Lee, T. Lee, H. K. Song, J. Cho, B. S. Kim, *Energy Environ. Sci.*, 2011, **4**, 4148—4154.
18. J. S. Lee, G. S. Park, H. I. Lee, S. T. Kim, R. Cao, M. Liu and J. Cho, *Nano Lett.*, 2011, **11**, 5362—5366.
19. J. Wang, H. Wu, D. Gao, S. Miao, G. Wang and X. Bao, *Nano Energy*, 2015, **13**, 387—396.
20. G. Nam, J. Park, M. Choi, P. Oh, S. Park, M. G. Kim, N. Park, J. Cho and J. S. Lee, *ACS nano*, 2015, **9**, 6493—6501.
21. Q. Liu, Y. B. Wang, L. M. Dai and J. N. Yao, *Adv. Mater.*, 2016, **28**, 3000—3006.
  
22. S. Zhu, Z. Chen, B. Li, D. Higgins, H. Wang, H. Li and Z. Chen, *Electrochim. Acta*, 2011, **56**, 5080—5084.
23. J. Zhang, Z. Zhao, Z. Xia and L. Dai, *Nat. Nanotech.*, 2015, **10**, 444—452.
24. Z. Chen, A. Yu, R. Ahmed, H. Wang, H. Li and Z. Chen, *Electrochim. Acta*, 2012, **69**, 295—300.
25. G. Du, X. Liu, Y. Zong, T. A. Hor, A. Yu, Z. Liu, *Nanoscale*, 2013, **5**, 4657—4661.
26. Z. Q. Liu, H. Cheng, N. Li, T. Y. Ma and Y. Z. Su, *Adv. Mater.*, 2016, **28**, 3777—3784.